Bioorganic & Medicinal Chemistry 23 (2015) 4583–4590

Contents lists available at ScienceDirect

Bioorganic & Medicinal Chemistry

journal homepage: www.elsevier.com/locate/bmc

Strong positive cooperativity in binding to the A_3T_3 repeat by Hoechst 33258 derivatives attaching the quinoline units at the end of a branched linker

Hironori Koda [a], John Alan Brazier [b], Ippei Onishi [a], Shigeki Sasaki [a,*]

[a] Graduate School of Pharmaceutical Sciences, Kyushu University, 3-1-1 Maidashi, Higashi-ku, Fukuoka 812-8582, Japan
[b] School of Pharmacy, University of Reading, Chemistry Building, Whiteknights, PO Box 224, Reading RG6 6AD, UK

ARTICLE INFO

Article history:
Received 28 April 2015
Revised 29 May 2015
Accepted 30 May 2015
Available online 16 June 2015

Keywords:
Cooperative binding
DNA repeat
Hoechst
Fluorescence titration
McGhee–von Hippel equation

ABSTRACT

Hoechst 33258 derivatives with additional interacting moieties attached at the ends of branched linkers were synthesized, and their DNA binding properties were investigated with regard to the A3T3 repeat by measuring fluorescence spectra. The binding property of the ligand was investigated by fluorescence titration, and the titration data were analyzed using the McGhee–von Hippel method. Ligand 6Q with the quinolin-6-yloxyacetyl group and Ligand IQ with isoquinolin-6-yloxyacetyl group at the ends of the branched linkers exhibit highly positive cooperativity for the DNA having 5 A3T3 sites with 3 base-insertions between them with sequence selectivity. The strategy developed in this study may be generally applicable for designing ligands for repetitive DNA sequences.

1. Introduction

Repetitive DNA sequences are widely distributed in genomes and have received considerable attention because of their diverse roles in structure and biology,[1–3] which include telomeric repeat[4] and trinucleotide repeat,[5] etc. Some diseases are associated with expansion disorders of trinucleotide repeat. For example, a trinucleotide (CAG) repeat in the androgen receptor gene lengthens from 13 to 30 repeats in the normal range to 40 or more repeats in patients with the disorder of this receptor. Disorders of repeat expansion cause loss of function or toxicity of proteins. Therefore, selective compounds for targeting expansion of trinucleotide repeat are desired for diagnostic and therapeutic purposes.[6] However, effective methods have not yet been developed. Triplex-forming oligonucleotides and minor groove binders are representative compounds for binding with duplex DNA. Nevertheless, expansion of a trinucleotide repeat exceeds a length for recognition of these compounds. In this study, we attempted to establish a new strategy in designing molecules for targeting expansion of a sequence repeat. From the perspective of small molecules, cooperativity is of great interest for expansion of a binding site. Certain small molecular compounds, such as peptides,[7] metal complexes,[8] intercalators,[9] and minor groove binders,[10] show cooperativity in binding with DNA; however, few studies have considered this approach for designing molecules for DNA repeat. Here, we describe that the Hoechst 33258 derivatives with the additional interaction units attached at the ends of a branched linker exhibit highly positive cooperativity for the binding with the A_3T_3 repeat.

2. Results and discussion

2.1. Molecular design

Figure 1 outlines our approach, in which additional interaction units are attached at the ends of a branched linker of the ligand to promote cooperativity between the adjacent ligands. It is well known that Hoechst 33258 produces bright fluorescence by binding to the minor groove of duplex DNA, with a marked preference for AT-rich regions.[11–14] Other binding modes are also observed, depending on such factors as the DNA sequence, ligand concentrations, and buffer conditions.[10,15–17] In our previous work,[18,19] Hoechst derivatives with the bipyridine unit were demonstrated to form bimolecular chelate complexes with the Cu(II) in the binding with DNA. In this study, we attempted to determine suitable interaction units at the ends of the branched linker to validate this concept for cooperative binding with the A_3T_3 repeat.

* Corresponding author. Tel./fax: +81 92 642 6615.
E-mail address: sasaki@phar.kyushu-u.ac.jp (S. Sasaki).

http://dx.doi.org/10.1016/j.bmc.2015.05.056
0968-0896/

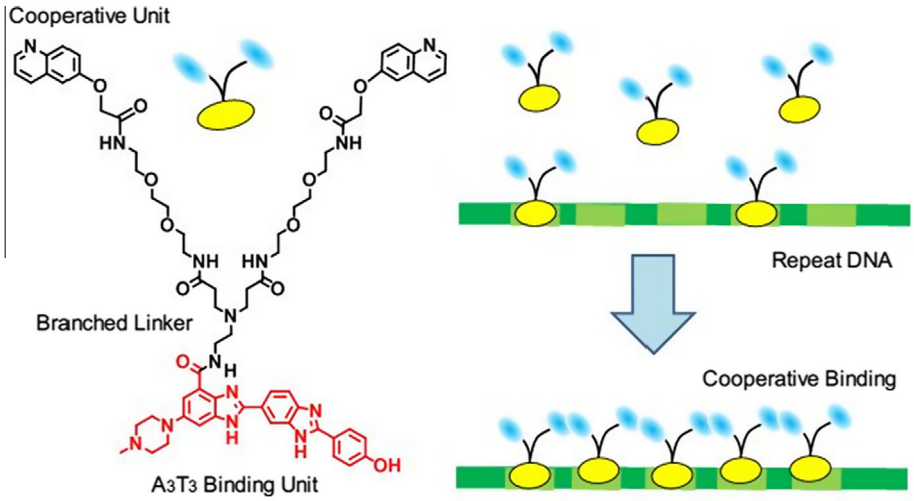

Figure 1. General strategy for cooperative binding to a repetitive DNA sequence.

2.2. Chemistry

Figure 2 summarizes the structure of the ligands and their components. The carboxy derivative of Hoechst 33258 (**1**)[18] was used as the key unit. The dipropionic acid derivative of ethylenediamine linker **2** was coupled with the mono-modified derivative of diamine spacers (**3**–**6**) using standard condensation reagents to give the corresponding branched linker. After deprotection of the Boc group, the branched linker was coupled with **1** to form Ligand X (see Supporting information for the synthetic procedures of the components). The synthesized ligands were purified by HPLC and quantified by ^{1}H NMR using maleic acid as an internal standard. The ligand is named for its terminal group and the linker; for example, Ligand 6Q is constructed of the branched linker with **3** (R = quinolin-6-yloxyacetyl attached at the terminal). Ligand 6QS contains the short spacer (**4**) at the ends of the branched linker, and 6QSL represents the case in which both the short (**4**) and long linkers (**6**) are conjugated. Ligand MonoQ was synthesized as the control ligand conjugating the non-branched quinolin-6-yloxyacetyl linker. For the DNA substrates, the A_3T_3 sequence was chosen as a favorable binding site for Hoechst 33258, and duplex DNA sequences with 60 base pairs in length were designed. DNA substrate is named for the numbers of A_3T_3 sites and the base insertions between them (Chart 1). For example, DNA5(3) is constructed of five A_3T_3 sites with three base insertion containing G and C. DNA5(1), DNA5(3) and DNA5(6) are different in the number of inserted bases between the A_3T_3 sites.

2.3. Binding evaluation by CD

Figure 3 presents examples of the CD spectral changes produced by the binding of Ligand 6Q with DNA1 and DNA5(3). The CD spectra of DNA1 did not show significant change by the addition of Ligand 6Q (Fig. 3A), although the complexes were formed as discussed in the following session. In contrast, DNA5(3) indicated significant CD changes by binding with Ligand 6Q (Fig. 3B). Isoelliptic points observed at 256 nm and 284 nm suggest a single mode of binding with respect to the complex structures responsible for the CD spectra. The CD bands are attributable to each structural component: bands approximately 260 nm for DNA-Hoechst binding, bands approximately 322 nm for 6-quinolinol, and bands approximately 370 nm for the Hoechst part. These results show that Ligand 6Q binding to DNA5(3) induces DNA conformational change. The titration profiles monitored at 275 nm and 327 nm were well fitted by non-linear least-squares to the theoretical curve calculated by assuming a 1:1 binding stoichiometry between Ligand 6Q and the A_3T_3 site, and the association constants were estimated to be $K_s = 6.5 \times 10^6\ M^{-1}$ for the change at 275 nm and $3.9 \times 10^5\ M^{-1}$ for the change at 327 nm. Ligand 6Q was used at μM concentrations for CD measurements, thereby forming typical minor groove binding with the A_3T_3 site. It turned out that it was difficult to evaluate binding cooperativity by CD measurement, therefore, we next performed the fluorescence titration experiments.

2.4. Fluorescent titration experiments

The binding property of the ligand was investigated by fluorescence titration using the ligand at a concentration of 10 nM. A portion of DNA solution was added to a buffer solution of the ligand, and the increase in fluorescence intensity was measured. Figure 4A represents examples obtained using Ligand 6Q and DNA5(3). As control binding experiments, the use of DNA0 did not increase the fluorescence intensity significantly; thus, the fluorescence titration data were first analyzed based on the binding to A_3T_3 sites. The titration results were well simulated using the non-linear curve-fitting method by assuming two binding modes, one with high affinity and the other with low affinity (Fig. 4A, circles: observed values, dotted line: calculated values). The titration data were analyzed using the McGhee–von Hippel method, which is an established method of analyzing the cooperativity in the binding of ligands with duplex DNA and is based on Eq. 1.[20,21] The McGhee–von Hippel analysis produces three parameters, n (the number of base pairs covered by one ligand), K (the association constant, M^{-1}), and ω (the cooperativity parameter). A large ω value corresponds to strong cooperativity due to higher ratio of the closely bound complexes. The mean cluster size C_n on the DNA substrate can be calculated by Eq. 2.[21–23]

At first, the complex concentration at each base-pair concentration was calculated from the titration data to produce the v (the concentration of the bound ligand per base pair) and v/L values (L is the free ligand concentration). The v/L values were plotted against the v values (Fig. 4B). These plots were fitted by non-linear curve-fitting method with the McGhee–von Hippel Eq. 1 to produce the three parameters, n, K, and ω. For the titration data obtained with Ligand 6Q, these parameters were determined to be $n = 19.3$, $K = 4.2 \times 10^3\ M^{-1}$, and $\omega = 2.5 \times 10^4$. It should be noted that a large ω value indicates a highly positive cooperativity for the binding of Ligand 6Q to DNA**5**(3).

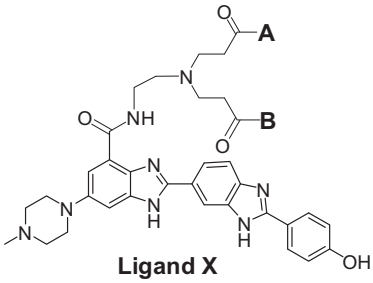

Ligand X

Ligand Name	Linker for A and B	Unit R of the linker **3**
NH_2	A=B: **3**	H
Ac		Acetyl
6Q		Quinolin-6-yloxyacetyl
Nac	A=B: **3**	Naphthalen-2-yloxyacetyl
Py		Pyridine-3-yloxyacetyl
IQ		Isoquinolin-6-yloxyacetyl
$6QNO_2$		5-Nitroquinolin-6-yloxyacetyl
6QBr		5-Bromoquinolin-6-yloxyacetyl
2Q		Quinolin-2-yloxyacetyl
6Qx		Quinoxalin-6-yloxyacetyl
6QS	A=B: **4**	
6QL	A=B: **5**	
6QSL	A: **6** , B: **4**	

Ligand MonoQ

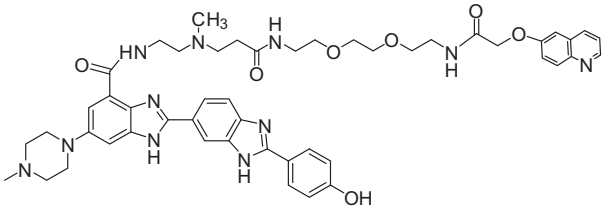

Componetns of Ligand X

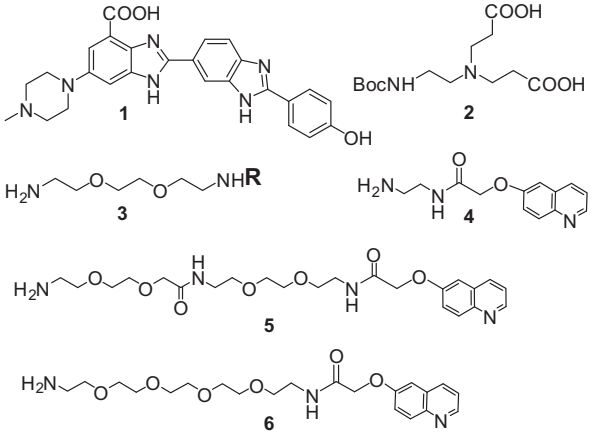

Figure 2. Structure of the ligands.

$$\frac{v}{L} = K\cdot(1-nv)\cdot\left(\frac{(2\omega+1)(1-nv)+v-R}{2(\omega-1)(1-nv)}\right)^{n-1}\cdot\left(\frac{1-(n+1)v+R}{2(1-nv)}\right)^{2} \quad (1)$$

$$C_n = \frac{2v(\omega-1)}{(n-1)v-1+R} \qquad R = \sqrt{[1-(n+1)v]^2+4\omega v(1-nv)} \quad (2)$$

The mean cluster number (C_n) at a v value was calculated using the n and ω parameters and is plotted against the [A_3T_3]/[Ligand] ratio in Figure 4C. The C_n values of Hoechst 33258 in binding to

DNA0
GCGCCGGATACGCCGGATACGGCGCCGACGGATCGCACGACGCACGACAGAGTCGATCGT -3′
CGCGGCCTATGCGGCCTATGCCGCGGCTGCCTAGCGTGCTGCGTGCTGTCTCAGCTAGCA -5′

DNA1
GCGCCGGATACGCCGGATACGGCGCCGAAATTTCGCACGACGCACGACAGAGTCGATCGT -3′
CGCGGCCTATGCGGCCTATGCCGCGGCTTTAAAGCGTGCTGCGTGCTGTCTCAGCTAGCA -5′

DNA5(1)
GCGCCGGATACGAAATTTGAAATTTCAAATTTCAAATTTGAAATTTCCCAGAGTCGATCG -3′
CGCGGCCTATGCTTTAAACTTTAAAGTTTAAAGTTTAAACTTTAAAGGGTCTCAGCTAGC -5′

DNA5(3)
GCGCCGAGCAAATTTGTCAAATTTGCGAAATTTACTAAATTTCGTAAATTTCCCAGTCGT -3′
CGCGGCTCGTTTAAACAGTTTAAACGCTTTAAATGATTTAAAGCATTTAAAGGGTCAGCA -5′

DNA5(6)
GCGAAATTTGGACCCAAATTTCGACGGAAATTTGCAGGGAAATTTCGTGACAAATTTCGT -3′
CGCTTTAAACCTGGGTTTAAAGCTGCCTTTAAACGTCCCTTTAAAGCACTGTTTAAAGCA -5′

Chart 1. DNA sequences used in this study.

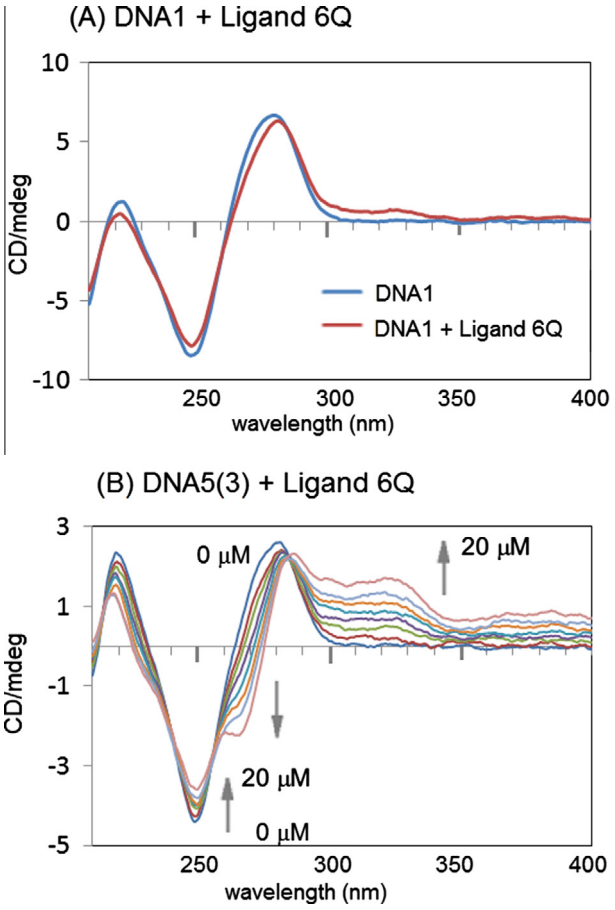

Figure 3. The spectral changes of Ligand 6Q and DNA5(3). (A) CD of DNA1 (5 μM in A_3T_3) and CD with Ligand 6Q (10 μM, 2 equiv for A_3T_3). (B) CD Titration of DNA5(3) (2 μM in A_3T_3) with Ligand 6Q (0–4 μM).

DNA1 were between 2 and 1, in good agreement with the known preference of Hoechst 33258 for the A_3T_3 sequence. Interestingly, large cluster formation is indicated for the binding of the ligand 6Q and DNA5(3), even at a high [A_3T_3]/[Ligand] ratio. The binding properties of other ligands were similarly evaluated to obtain three parameters (Table S1). The ω cooperative parameters obtained with a variety of ligands are compared in Figure 5.

Hoechst 33258 exhibited little cooperativity to DNA, regardless of the number of A_3T_3 binding sites, as expected. The ligands 6Q exhibited the highest selective cooperativity for DNA**5**(3). The ligands NH_2, Ac MonoQ did not display marked cooperativity, indicating that the two quinoline parts at the end of the branched linker are essential for high cooperativity. The ω cooperativity

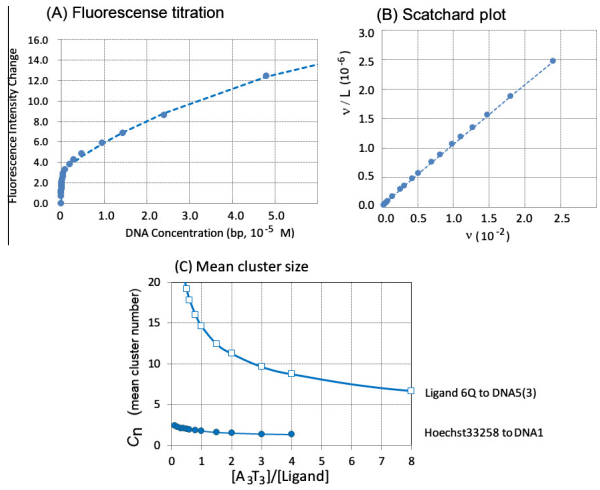

Figure 4. The fluorescence titration of the ligand 6Q by DNA**5**(3). (A) Circles represent raw data of titration, which are well fitted to the dotted line calculated by using the three parameters. (B) The Scatchard plot of ν and ν/L. Three parameters, n, K, and ω, which were obtained using Eq. 1, were used to calculate the dotted line. (C) The mean cluster sizes (C_n) were calculated using Eq. 2. Hoechst 33258 binding to DNA**1** (closed circles and blue line) and the ligand 6Q binding to DNA**5**(3) (open squares and blue line) are plotted against the $[A_3T_3]/[Ligand]$ ratio.

parameter of the ligand 6Q for DNA**5**(3) was the largest in this study. The linker length of 6Q seems to be fitted to DNA**5**(3), and the interval of a single base pair in DNA5(1) and six base pairs in DNA**5**(6) may be shorter or longer to maintain mutual contact of the ligand 6Q. 6QL with the longer spacer, 6QS with the short spacer and 6QSL with both the short and long spacers did not exhibit marked cooperativity. Therefore, the symmetrical linker structure with an appropriate spacer length is crucial for 6Q to exhibit cooperativity (Fig. 5A).

Interestingly, among the structurally resembling ligands, only IQ exhibited cooperativity with selectivity to DNA5(3) (Fig. 5B). Ligand Nac, which has a naphthalene-2-ol unit, exhibited cooperativity to some extent, albeit with no sequence selectivity. It should be noted that decrease in cooperativity and selectivity of Ligand Nac arose from the absence of ring nitrogen in naphthalene. The 5-nitro and 5-bromo substitution of the quinoline ring largely diminished cooperativity. The low cooperativity with 6Qx, 2Q, or Py indicated the importance of the positions of the nitrogen atom of the quinoline ring.

The quinoline ring is well known to produce molecular interactions, such as π–π stacking,[24,25] binding with metal cations[26] and hydrogen bonding.[27] In aqueous media, the π–π interactions are presumably major assembling forces, which may occur through dipole-dipole interactions between quinolines.[21,28,29] Substitution pattern of the quinoline ring produces the different dipole moments, which might be beneficial in the case of Ligand 6Q and IQ for the high cooperativity.

The UV–vis absorption bands of Ligand 6Q were shifted by binding with DNA5(3); the Hoechst region shifted to longer wavelength (372.5 to 384.5 nm) with 50% increased absorbance, the quinoline region shifted to shorter wavelength (328.5 to 326.5 nm) with 43%

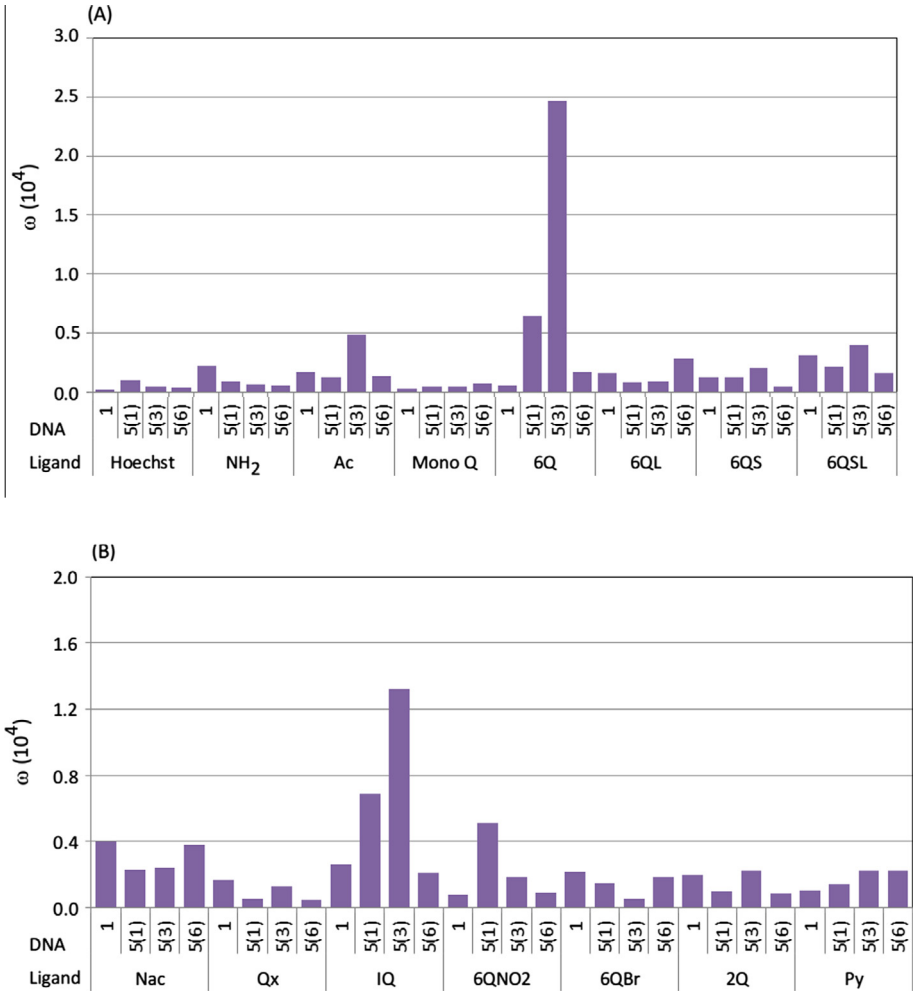

Figure 5. Comparison of the cooperativity parameter (ω).

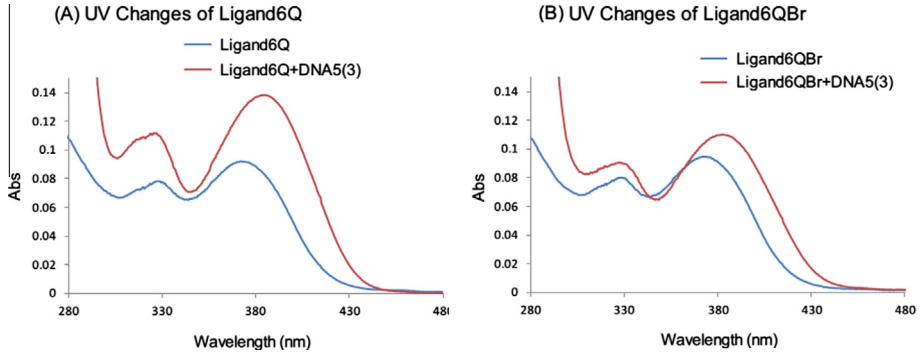

Figure 6. UV change of Ligand 6Q (A) and Ligand 6QBr (B) by binding with DNA5(3).

increased absorbance (Fig. 6A). These UV changes suggest strong tendencies of the Hoechst parts for forming *J*-aggregates and the quinoline parts for *H*-type aggregates. In contrast, although Ligand 6QBr showed similar wavelength shifts for both regions, their absorbance increases were smaller; 13% for the bromoquinoline part and 16% for the Hoechst part (Fig. 6B). Accordingly, Ligand 6QBr has less ability for the formation of both *J*- and *H*-aggregates. The difference of Ligand 6Q and 6QBr in cooperativity may be explained based on their different ability for *J*- and *H*-aggregates formation. It has been reported that, in addition to a representative minor groove binding mode, Hoechst 33258 binds to DNA with multiple stoichiometries including stacking aggregates depending on the concentration and buffer conditions.[11] Thus, it is conceivable that the ligand molecules bound in the minor groove promote interactions between the quinoline units, which in turn facilitate stacking aggregate formation of the ligand molecules. Further study on the complex structure is needed for detail discussion about the effect of the terminal binding parts on the cooperativity.

3. Conclusions

In conclusion, this study clearly demonstrated that the ligand 6Q and IQ with quinoline moieties at the ends of the branched linkers exhibit highly positive cooperativity with sequence selectivity. Although it is difficult to observe detailed complex structure, the cluster formation has been supported by fluorescence titration and UV–vis measurements. The strategy developed in this study may be generally applicable for designing ligands for repetitive DNA sequences. Potential application of selective ligands for the expanded DNA repeats include intracellular imaging of DNA and interference of transcription of the gene, which are now ongoing in our group.

4. Experimental

4.1. Chemical synthesis

4.1.1. General

^{1}H NMR (400 MHz) and ^{13}C NMR (100, 125, 150 MHz) spectra were recorded on a Varian UNITY-400 or INOVA-500. Infrared (IR) spectra were obtained using a SHIMADZU FTIR-8400 spectrometer. High resolution mass spectra analyses were recorded on an Applied Biosystems Mariner System 5299 spectrometer using bradykinin, neurotensin, and angiotensin as an internal standard. See Supplementary data for the synthesis of the components (**1**–**6**).

4.1.2. Synthesis of Ligand 6Q as a general procedure for the synthesis of the ligand

Quinolin-6-yloxyacetyl derivative of 1,2-bis(2-aminoethoxy)-ethane (**3**, R = Quinolin-6-yloxyacetyl) (2∼3 equiv), HBTU (2.2 equiv), DIPEA (12 equiv) and HBT (2.2 equiv) were added to a solution of *N*-Boc derivative of the ethylenediamine linker **2** in DMF (0.30 M) at room temperature under argon, and the reaction mixture was stirred at room temperature. After the completion of the reaction, the reaction mixture was evaporated, and the residue was diluted with dichloromethane. The mixture was washed with saturated aqueous $NaHCO_3$ solution and brine. The organic layer was dried over anhydrous Na_2SO_4, filtered and evaporated. The residue was purified by column chromatography (Kanto 60N, dichloromethane/methanol) to afford the corresponding *N*-Boc linker derivative. Trifluoroacetic acid (20 equiv) was added to a solution of the *N*-Boc linker derivative in dichloromethane, and the reaction mixture was stirred at room temperature. After the completion of the reaction, the reaction mixture was evaporated. The crude product was dissolved in DMF (0.10 M) and used for the next reaction without purification. Hoechst-COOH (**1**) (1.1 equiv), HBTU (1.1 equiv), HBT (1.1 equiv) and DIPEA (12 equiv) were added to the above solution under argon. The reaction mixture was stirred at room temperature. After the completion of the reaction, the reaction mixture was evaporated. The residue was purified by column chromatography (Fujisilysia NH, chloroform/methanol eluent) to afford Ligand 6Q. Analytical sample was obtained by reverse-phase HPLC (Nacalai Tesque COSMOSIL 5C18-AR-II 10 mm × 250 mm; eluents H_2O (A) and CH_3CN (B); gradient 0–20 min, 15–100% B in A + B; flow rate 2.5 mL/min; detection 368 nm). The ligand concentration was determined by the integral values of ^{1}H NMR spectrum including maleic acid as the internal standard.

4.1.3. Ligand 6Q

An orange solid. IR (cm^{-1}) 3285.7, 3091.4, 1671.4, 1200.1, 1130.1; ^{1}H NMR (400 MHz, CD_3OD) δ (ppm) 8.78 (dd, J = 4.8, 1.5 Hz, 2H), 8.52 (d, J = 8.2 Hz, 2H), 8.48 (d, J = 0.9 Hz, 1H), 8.33 (dd, J = 8.6, 1.5 Hz, 1H), 8.00 (d, J = 8.9 Hz, 2H), 7.98 (d, J = 9.2 Hz, 2H), 7.81 (d, J = 8.9 Hz, 1H), 7.71 (d, J = 2.1 Hz, 1H), 7.66 (dd, J = 8.5, 4.9 Hz, 2H), 7.61 (dd, J = 9.1, 2.7 Hz, 2H), 7.37 (d, J = 2.7 Hz, 2H), 7.34 (d, J = 2.4 Hz, 1H), 7.05 (d, J = 8.9 Hz, 2H), 4.63 (s, 4H), 4.03 (s, 2H), 3.63–3.58 (m, 8H), 3.53–3.48 (m, 12H), 3.46–3.40 (m, 10H), 3.34–3.32 (m, 4H), 3.16 (t, J = 5.3 Hz, 4H), 3.01 (s, 3H), 2.80 (t, J = 6.3 Hz, 4H); ^{13}C NMR (125 MHz, CD_3OD) δ (ppm) 172.1, 169.9, 169.2, 164.4, 159.0, 157.0, 153.2, 152.4, 148.2, 144.7, 144.5, 138.1, 137.4, 135.2, 134.3, 131.8, 131.2, 128.0, 126.0, 124.9, 123.2, 122.4, 117.9, 116.4, 115.3, 114.7, 113.6, 108.8, 104.8, 71.2, 70.3, 70.2, 68.5, 54.8, 52.1, 43.6, 40.3, 40.0, 36.5, 29.7; HRESI-MS (m/z) calcd for $C_{68}H_{80}N_{14}O_{12}$ ($[M+2H]^{2+}$) 643.3113, found 643.3123.

4.1.4. Ligand NH_2

The title compound was prepared as a yellow solid. IR (cm^{-1}) 3432.4, 1675.0, 1202.4, 1133.6; ^{1}H NMR (400 MHz, CD3OD) δ (ppm) 8.50 (s, 1H), 8.26 (d, J = 7.3 Hz, 1H), 8.03 (d, J = 8.9 Hz, 2H),

7.79 (d, J = 8.5 Hz, 1H), 7.73 (d, J = 2.1 Hz, 1H), 7.39 (d, J = 2.4 Hz, 1H), 7.02 (d, J = 8.5 Hz, 2H), 4.03 (t, J = 5.6 Hz, 2H), 3.63 (t, J = 5.6 Hz, 2H), 3.60–3.56 (m, 12H), 3.52–3.50 (m, 6H), 3.38 (t, J = 5.6 Hz, 4H), 3.22 (t, J = 5.6 Hz, 6H), 3.08 (t, J = 5.2 Hz, 4H), 3.01 (s, 3H), 2.82 (t, J = 6.4 Hz, 4H); ^{13}C NMR (150 MHz, CD3OD) δ (ppm) 172.3, 169.5, 163.0, 151.1, 147.9, 138.7, 130.5, 119.1, 117.5, 117.2, 116.0, 105.0, 71.3, 71.2, 70.4, 67.9, 54.9, 54.4, 52.1, 45.2, 43.6, 40.6, 40.2, 36.5, 29.8; HRESI-MS (m/z) calcd for $C_{46}H_{66}N_{12}O_8$ ($[M+2H]^{2+}$) 458.2636, found 458.2672.

4.1.5. Ligand Ac

The title compound was obtained as an orange solid. IR (cm^{-1}) 3286.0, 3089.9, 2876.3, 1669.7, 1196.7, 1134.4; ^{1}H NMR (400 MHz, CD_3OD) δ (ppm) 8.56 (s, 1H), 8.38 (d, J = 8.2 Hz, 1H), 8.04 (d, J = 8.9 Hz, 2H), 7.85 (d, J = 8.5 Hz, 1H), 7.74 (d, J = 2.4 Hz, 1H), 7.40 (d, J = 2.1 Hz, 1H), 7.07 (d, J = 8.9 Hz, 2H), 4.04 (s, 2H), 3.63–3.58 (m, 8H), 3.50–3.41 (m, 16H), 3.30–3.27 (m, 10H), 3.12 (t, J = 5.2 Hz, 4H), 3.02 (s, 3H), 2.80 (t, J = 5.5 Hz, 4H), 1.90 (s, 6H); ^{13}C NMR (125 MHz, CD_3OD) δ (ppm) 173.4, 172.2, 169.3, 164.4, 153.2, 152.6, 148.2, 138.2, 135.3, 134.4, 131.2, 127.3, 126.1, 122.5, 117.9, 116.4, 115.2, 114.8, 113.6, 104.9, 71.2, 70.5, 70.2, 54.8, 54.6, 52.1, 43.6, 43.6, 40.3, 40.2, 36.5, 29.6, 22.6; HRMS (m/z) calcd for $C_{50}H_{70}N_{12}O_{10}$ ($[M+H]^+$) 999.5411, found 999.5402.

4.1.6. Ligand Nac

Ligand Nac was obtained as a yellow solid. IR (cm^{-1}) 3070.1, 2866.9, 1667.6, 1200.2, 1183.3, 1128.7; ^{1}H NMR (400 MHz, CD_3OD) δ (ppm) 8.43 (d, J = 0.9 Hz, 1H), 8.31 (dd, J = 8.5, 1.5 Hz, 1H), 7.98 (dd, J = 7.8, 2.1 Hz, 2H), 7.76 (d, J = 8.6 Hz, 1H), 7.72–7.70 (m, 3H), 7.68 (s, 2H), 7.64 (d, J = 8.2 Hz, 2H), 7.37–7.32 (m, 3H), 7.29–7.24 (m, 2H), 7.13 (dd, J = 8.9, 2.4 Hz, 2H), 7.10 (d, J = 2.4 Hz, 2H), 7.05 (dd, J = 7.8, 2.1 Hz, 2H), 4.53 (s, 4H), 3.90 (t, J = 5.2 Hz, 2H), 3.56 (t, J = 5.2 Hz, 2H), 3.52-3.44 (m, 16H), 3.41–3.35 (m, 12H), 3.27 (t, J = 5.2 Hz, 4H), 3.13 (t, J = 5.2 Hz, 4H), 2.98 (s, 3H), 2.75 (t, J = 6.1 Hz, 4H); ^{13}C NMR (125 MHz, CD_3OD) δ (ppm) 172.0, 171.0, 169.3, 164.2, 156.7, 153.0, 152.7, 148.0, 138.2, 135.7, 135.3, 134.5, 131.1, 130.7, 130.6, 130.6, 128.6, 127.9, 127.5, 125.8, 125.1, 122.3, 119.3, 117.8, 116.3, 115.0, 113.3, 108.4, 108.3, 71.2, 71.2, 70.4, 70.2, 68.1, 54.7, 52.0, 43.6, 40.3, 39.9, 36.5, 29.7; HRESI-MS (m/z) calcd for $C_{70}H_{82}N_{12}O_{12}$ ($[M+2H]^{2+}$) 642.3160, found 642.3174.

4.1.7. Ligand 2Q

Ligand 2Q was obtained as a yellow solid. IR (cm^{-1}) 3275.3, 3088.0, 1647.2, 1199.9, 1129.1; ^{1}H NMR (400 MHz, CD_3OD) δ (ppm) 8.46 (s, 1H), 8.31 (dd, J = 8.6, 1.5 Hz, 1H), 7.99 (d, J = 8.9 Hz, 2H), 7.82 (d, J = 9.8 Hz, 2H), 7.79 (d, J = 8.5 Hz, 1H), 7.69 (d, J = 2.1 Hz, 1H), 7.60 (d, J = 7.9 Hz, 2H), 7.52 (t, J = 7.9 Hz, 2H), 7.32 (d, J = 2.1 Hz, 1H), 7.28 (d, J = 8.9 Hz, 2H), 7.23 (t, J = 7.6 Hz, 2H), 7.04 (d, J = 8.9 Hz, 2H), 6.61 (d, J = 9.5 Hz, 2H), 4.99 (s, 4H), 4.01 (t, J = 5.5 Hz, 2H), 3.64–3.54 (m, 10H), 3.49–3.39 (m, 10H), 3.36–3.34 (m, 6H), 3.28–3.27 (m, 2H), 3.11 (t, J = 5.5 Hz, 4H), 2.97 (s, 3H), 2.78 (t, J = 6.1 Hz, 4H); ^{13}C NMR (125 MHz, CD_3OD) δ (ppm) 179.3, 172.1, 169.8, 169.4, 164.2, 163.8, 153.5, 153.0, 147.9, 142.0, 142.0, 140.7, 138.4, 132.2, 130.9, 130.2, 127.2, 125.4, 123.9, 122.3, 121.3, 117.7, 116.1, 115.5, 113.6, 98.9, 71.3, 71.2, 70.4, 70.2, 54.8, 52.1, 46.2, 43.6, 40.5, 40.3, 36.6, 29.7; HRESI-MS (m/z) calcd for $C_{68}H_{80}N_{14}O_{12}$ ($[M+2H]^{2+}$) 643.3113, found 643.3080.

4.1.8. Ligand IQ

Ligand IQ was obtained as an orange solid. IR (cm^{-1}) 3283.7, 3079.1, 1671.4, 1200.9, 1133.9; ^{1}H NMR (400 MHz, CD_3OD) δ (ppm) 9.36 (s, 2H), 8.43 (s, 1H), 8.35 (d, J = 6.4 Hz, 2H), 8.25 (d, J = 9.5 Hz, 2H), 8.22 (s, 1H), 8.07 (d, J = 6.4 Hz, 2H), 7.98 (d, J = 8.9 Hz, 2H), 7.75 (d, J = 8.6 Hz, 1H), 7.69 (d, J = 2.1 Hz, 1H), 7.57 (dd, J = 9.2, 2.4 Hz, 2H), 7.44 (d, J = 2.1 Hz, 2H), 7.33 (d, J = 2.1 Hz, 1H), 6.99 (d, J = 8.5 Hz, 2H), 4.73 (s, 4H), 4.04 (s, 2H), 3.66–3.58 (m, 10H), 3.53–3.49 (m, 12H), 3.45–3.40 (m, 10H), 3.23–3.20 (m, 2H), 3.17 (t, J = 5.5 Hz, 4H), 3.02 (s, 3H), 2.83 (t, J = 6.3 Hz, 4H); ^{13}C NMR (125 MHz, CD_3OD) δ (ppm) 172.2, 169.4, 165.4, 164.4, 148.2, 146.6, 142.9, 133.6, 132.7, 131.2, 126.6, 126.0, 125.2, 124.9, 124.6, 122.4, 117.9, 116.3, 115.3, 113.6, 107.9, 71.2, 70.3, 70.2, 68.5, 54.7, 52.1, 43.6, 40.3, 40.0, 36.5, 29.7; HRESI-MS (m/z) calcd for $C_{68}H_{80}N_{14}O_{12}$ ($[M+2H]^{2+}$) 643.3113, found 643.3158.

4.1.9. Ligand Py

Ligand Py was obtained as an orange solid. IR (cm^{-1}) 3275.3, 1672.8, 1200.1, 1131.0; ^{1}H NMR (400 MHz, CD3OD) δ (ppm) 8.57 (s, 1H), 8.40 (dd, J = 8.7, 1.5 Hz, 1H), 8.35 (d, J = 2.8 Hz, 2H), 8.24 (dd, J = 4.9, 1.2 Hz, 2H), 8.05 (d, J = 8.9 Hz, 2H), 7.86 (d, J = 8.2 Hz, 1H), 7.74 (d, J = 2.4 Hz, 1H), 7.61 (ddd, J = 8.6, 2.7, 1.2 Hz, 2H), 7.51 (dd, J = 8.7, 4.9 Hz, 2H), 7.39 (d, J = 2.4 Hz, 1H), 7.08 (d, J = 8.9 Hz, 2H), 4.62 (s, 4H), 4.04 (t, J = 5.2 Hz, 2H), 3.65–3.58 (m, 8H), 3.51–3.46 (m, 12H), 3.44–3.39 (m, 10H), 3.21 (t, J = 7.3 Hz, 2H), 3.20 (t, J = 7.3 Hz, 2H), 3.14 (t, J = 5.2 Hz, 4H), 3.02 (s, 3H), 2.81 (t, J = 6.3 Hz, 4H); ^{13}C NMR (125 MHz, CD3OD) δ (ppm) 172.2, 169.7, 169.3, 164.4, 157.0, 153.3, 152.7, 148.2, 140.0, 138.3, 135.5, 131.2, 128.0, 127.4, 126.0, 122.5, 117.9, 116.4, 115.3, 115.1, 113.6, 104.9, 103.9, 71.2, 70.3, 70.2, 68.6, 54.8, 54.6, 52.1, 43.6, 40.3, 40.0, 36.5, 29.6; HRESI-MS (m/z) calcd for $C_{60}H_{76}N_{14}O_{12}$ ($[M+2H]^{2+}$) 593.2956, found 593.2968.

4.1.10. Ligand 6QBr

Ligand 6QBr was obtained as an orange solid. IR (cm^{-1}) 3274.6, 3095.7, 1669.4, 1198.8, 1133.0; ^{1}H NMR (400 MHz, CD_3OD) δ (ppm) 8.73 (dd, J = 4.4, 1.4 Hz, 2H), 8.57 (d, J = 8.9 Hz, 2H), 8.43 (s, 1H), 8.32 (dd, J = 8.7, 1.4 Hz, 1H), 7.99 (d, J = 8.9 Hz, 2H), 7.94 (d, J = 9.2 Hz, 2H), 7.78 (d, J = 8.5 Hz, 1H), 7.67 (d, J = 2.1 Hz, 1H), 7.58 (dd, J = 8.7, 4.4 Hz, 2H), 7.54 (d, J = 9.2 Hz, 2H), 7.30 (d, J = 2.1 Hz, 1H), 7.06 (d, J = 8.9 Hz, 2H), 4.68 (s, 4H), 4.01 (t, J = 5.5 Hz, 2H), 3.64–3.58 (m, 8H), 3.56–3.52 (m, 10H), 3.48–3.42 (m, 10H), 3.38–3.34 (m, 6H), 3.19 (t, J = 5.5 Hz, 4H), 3.02 (s, 3H), 2.82 (t, J = 6.1 Hz, 4H); ^{13}C NMR (125 MHz, CD_3OD) δ (ppm) 172.2, 170.0, 169.2, 164.5, 154.2, 153.1, 152.5, 149.4, 148.1, 143.9, 138.1, 137.4, 135.1, 134.3, 131.2, 129.8, 129.5, 126.0, 124.0, 122.3, 120.2, 117.9, 116.3, 115.2, 114.7, 113.4, 109.3, 104.8, 71.3, 70.4, 70.3, 69.7, 54.8, 52.3, 43.6, 40.3, 40.0, 36.7, 30.7, 29.7; HRESI-MS (m/z) calcd for $C_{68}H_{78}N_{14}O_{12}Br_2$ ($[M+2H]^{2+}$) 721.2218, found 721.2261.

4.1.11. Ligand 6QNO$_2$

Ligand 6QNO$_2$ was obtained as a yellow solid. IR (cm^{-1}) 3303.4, 3088.3, 1667.6, 1185.6, 1131.4; ^{1}H NMR (400 MHz, CD_3OD) δ (ppm) 8.77 (dd, J = 4.3, 1.5 Hz, 2H), 8.43 (s, 1H), 8.30 (dd, J = 8.6, 1.5 Hz, 1H), 8.10 (d, J = 9.5 Hz, 2H), 8.08 (d, J = 8.6 Hz, 2H), 7.99 (d, J = 8.9 Hz, 2H), 7.77 (d, J = 8.6 Hz, 1H), 7.68 (d, J = 2.1 Hz, 1H), 7.62 (d, J = 9.5 Hz, 2H), 7.55 (dd, J = 8.9, 4.3 Hz, 2H), 7.32 (d, J = 2.4 Hz, 1H), 7.07 (d, J = 8.9 Hz, 2H), 4.73 (s, 4H), 4.02 (t, J = 5.8 Hz, 2H), 3.66–3.58 (m, 8H), 3.53–3.49 (m, 10H), 3.48–3.45 (m, 6H), 3.39 (t, J = 5.3 Hz, 4H), 3.36–3.32 (m, 6H), 3.17 (t, J = 5.3 Hz, 4H), 3.02 (s, 3H), 2.82 (t, J = 5.8 Hz, 4H); ^{13}C NMR (125 MHz, CD_3OD) δ (ppm) 172.1, 169.4, 169.2, 164.4, 153.1, 152.5, 151.0, 149.2, 148.1, 143.4, 138.2, 136.0, 135.1, 134.7, 134.3, 131.2, 131.0, 127.3, 125.9, 125.1, 122.4, 122.3, 119.3, 117.9, 116.3, 115.1, 114.8, 113.4, 104.8, 71.3, 71.2, 70.3, 70.3, 69.6, 54.8, 54.6, 52.2, 43.6, 40.3, 40.1, 36.6, 30.7, 29.7; HRESI-MS (m/z) calcd for $C_{68}H_{78}N_{16}O_{16}$ ($[M+2H]^{2+}$) 688.2964, found 688.2930.

4.1.12. Ligand 6Qx

Ligand 6Qx was obtained as a yellow solid. IR (cm^{-1}) 3271.9, 3077.9, 1668.1, 1199.9, 1128.0; ^1H NMR (400 MHz, CD_3OD) δ (ppm) 8.70 (d, J = 1.8 Hz, 2H), 8.63 (d, J = 1.8 Hz, 2H), 8.38 (s, 1H), 8.22 (d, J = 8.5 Hz, 1H), 7.98 (d, J = 8.6 Hz, 2H), 7.90 (d, J = 9.5 Hz, 2H), 7.73 (d, J = 8.5 Hz, 1H), 7.67 (d, J = 2.4 Hz, 1H), 7.48 (dd, J = 9.2, 2.7 Hz, 2H), 7.29 (d, J = 2.1 Hz, 1H), 7.26 (d, J = 2.7 Hz, 2H), 7.01 (d, J = 8.9 Hz, 2H), 4.62 (s, 4H), 4.03 (t, J = 5.5 Hz, 2H), 3.63–3.58 (m, 10H), 3.52–3.46 (m, 12H), 3.42-3.39 (m, 10H), 3.33–3.32 (m, 2H), 3.16 (t, J = 5.5 Hz, 4H), 3.02 (s, 3H), 2.82 (t, J = 6.3 Hz, 4H); ^{13}C NMR (125 MHz, CD_3OD) δ (ppm) 172.1, 170.2, 169.5, 163.1, 160.1, 154.4, 147.8, 146.5, 145.2, 144.2, 140.2, 131.3, 130.5, 124.4, 117.5, 116.0, 115.3, 109.0, 71.2, 71.2, 70.4, 70.2, 68.4, 54.9, 54.7, 52.2, 43.6, 40.3, 40.0, 36.6, 29.8; HRESI-MS (m/z) calcd for $C_{66}H_{78}N_{16}O_{12}$ ($[M+2H]^{2+}$) 644.3065, found 644.3081.

4.1.13. Ligand 6QL

IR (cm^{-1}) 3294.5, 3078.2, 1666.9, 1184.6, 1129.8; ^1H NMR (400 MHz, CD_3OD) δ (ppm) 8.83 (dd, J = 4.9, 1.5 Hz, 2H), 8.61 (d, J = 8.2 Hz, 2H), 8.51 (s, 1H), 8.36 (dd, J = 8.6, 1.5 Hz, 1H), 8.03 (d, J = 3.1 Hz, 2H), 8.01 (d, J = 2.4 Hz, 2H), 7.83 (d, J = 8.5 Hz, 1H), 7.73 (d, J = 5.2 Hz, 1H), 7.71 (d, J = 5.2 Hz, 2H), 7.67 (dd, J = 9.5, 2.8 Hz, 2H), 7.44 (d, J = 2.8 Hz, 2H), 7.35 (d, J = 2.1 Hz, 1H), 7.06 (d, J = 8.9 Hz, 2H), 5.76 (s, 4H), 4.04 (s, 2H), 3.92 (s, 4H), 3.64–3.59 (m, 8H), 3.57–3.52 (m, 16H), 3.52–3.48 (m, 8H), 3.48–3.43 (m, 10H), 3.38–3.35 (m, 8H), 3.16 (t, J = 6.4 Hz, 4H), 3.02 (s, 3H), 2.82 (t, J = 6.4 Hz, 4H); ^{13}C NMR (150 MHz, CD3OD) δ (ppm) 172.7, 172.2, 170.0, 169.2, 164.4, 162.6, 158.9, 153.2, 152.5, 148.2, 144.7, 144.4, 138.1, 137.8, 135.3, 134.5, 131.8, 131.2, 127.8, 126.0, 125.2, 123.3, 122.4, 117.9, 116.3, 115.3, 113.6, 108.8, 104.8, 71.8, 71.3, 70.4, 70.4, 70.2, 68.5, 54.8, 54.6, 52.1, 43.6, 40.3, 40.1, 39.9, 39.8, 36.5, 30.7, 29.6; HRESI-MS (m/z) calcd for $C_{80}H_{102}N_{16}O_{18}$ ($[M+2H]^{2+}$) 788.3852, found 788.3831.

4.1.14. Ligand 6QS

IR (cm^{-1}) 3282.4, 3094.7, 1667.9, 1185.8, 1128.4; ^1H NMR (400 MHz, CD3OD) δ (ppm) 8.65 (dd, J = 6.7, 1.5 Hz, 2H), 8.36 (s, 2H), 8.34 (s, 1H), 8.27 (d, J = 8.5 Hz, 1H), 7.91 (d, J = 8.9 Hz, 2H), 7.88 (d, J = 9.5 Hz, 2H), 7.76 (d, J = 8.2 Hz, 1H), 7.66 (d, J = 2.4 Hz, 1H), 7.53 (dd, J = 9.3, 5.2 Hz, 2H), 7.50 (dd, J = 9.7, 2.7 Hz, 2H), 7.30 (d, J = 2.1 Hz, 1H), 7.21 (d, J = 2.4 Hz, 2H), 7.01 (d, J = 8.9 Hz, 2H), 4.51 (s, 4H), 4.02 (s, 2H), 3.64–3.56 (m, 10H), 3.26–3.16 (m, 12H), 3.02 (s, 3H), 2.81 (s, 4H); ^{13}C NMR (150 MHz, CD3OD) δ (ppm) 172.8, 170.0, 169.2, 164.3, 162.7, 158.5, 152.9, 152.3, 148.1, 144.7, 143.8, 137.9, 135.1, 134.3, 131.6, 131.1, 127.4, 125.8, 125.3, 123.1, 122.2, 117.8, 116.1, 115.2, 114.7, 113.3, 108.5, 104.7, 68.2, 55.1, 54.8, 52.2, 43.6, 40.3, 39.7, 36.9, 30.7, 29.9; HRESI-MS (m/z) calcd for $C_{60}H_{64}N_{14}O_8$ ($[M+2H]^{2+}$) 555.2589, found 555.2576.

4.1.15. Ligand 6QSL

IR (cm^{-1}) 3272.2, 3091.0, 1669.4, 1199.5, 1185.4, 1129.4; ^1H NMR (400 MHz, CD_3OD) δ (ppm) 8.74 (dd, J = 4.7, 1.5 Hz, 1H), 8.63 (dd, J = 4.7, 1.5 Hz, 1H), 8.43 (s, 1H), 8.41 (s, 1H), 8.30 (s, 1H), 8.26 (dd, J = 8.5, 1.5 Hz, 1H), 7.95 (dd, J = 8.8, 2.8 Hz, 2H), 7.87 (d, J = 9.2 Hz, 1H), 7.76 (d, J = 8.9 Hz, 1H), 7.66 (d, J = 2.4 Hz, 1H), 7.58 (dd, J = 8.5, 4.4 Hz, 1H), 7.56 (dd, J = 9.5, 2.6 Hz, 1H), 7.49 (dd, J = 7.6, 3.8 Hz, 1H), 7.46 (dd, J = 9.6, 2.7 Hz, 1H), 7.31 (d, J = 2.4 Hz, 2H), 7.18 (d, J = 2.8 Hz, 1H), 7.02 (d, J = 8.9 Hz, 2H), 4.61 (s, 2H), 4.50 (s, 2H), 4.02 (s, 2H), 3.62–3.52 (m, 20H), 3.48–3.47 (m, 4H), 3.46–3.37 (m, 6H), 3.25 (t, J = 5.8 Hz, 2H), 3.23–3.18 (m, 4H), 3.09 (s, 2H), 3.01 (s, 3H), 2.80 (t, J = 5.8 Hz, 4H); ^{13}C NMR (125 MHz, CD3OD) δ (ppm) 172.7, 172.2, 170.3, 170.2, 169.3, 163.9, 162.7, 158.1, 157.9, 153.4, 152.8, 148.0, 146.6, 141.3, 140.9, 138.2, 136.0, 135.3, 131.3, 131.2, 130.9, 127.5, 127.1, 126.0, 125.8, 125.5, 123.1, 123.0, 122.3, 117.7, 116.1, 115.3, 113.6, 108.5, 108.3, 104.9, 71.5, 71.5, 71.4, 71.2, 71.1, 70.3, 70.1, 68.4, 68.2, 54.9, 54.8, 52.3, 52.1, 43.6, 40.3, 40.1, 39.7, 36.8, 29.9, 29.6, 24.1; HRESI-MS (m/z) calcd for $C_{68}H_{80}N_{14}O_{12}$ ($[M+2H]^{2+}$) 643.3113, found 643.3098.

4.1.16. Ligand MonoQ

IR (cm^{-1}) 3247.0, 3073.3, 1669.2, 1186.4, 1131.1; ^1H NMR (400 MHz, CD_3OD) δ (ppm) 8.89 (dd, J = 5.2, 1.2 Hz, 1H), 8.77 (d, J = 8.5 Hz, 1H), 8.53 (s, 1H), 8.38 (dd, J = 8.9, 1.5 Hz, 1H), 8.08 (d, J = 9.5 Hz, 1H), 8.04 (d, J = 9.2 Hz, 2H), 7.88 (d, J = 8.6 Hz, 1H), 7.83 (dd, J = 8.2, 5.2 Hz, 1H), 7.76 (d, J = 2.1 Hz, 1H), 7.74 (dd, J = 10.1, 2.7 Hz, 1H), 7.49 (d, J = 2.7 Hz, 1H), 7.38 (d, J = 2.1 Hz, 1H), 7.08 (d, J = 8.9 Hz, 2H), 4.67 (s, 2H), 4.03 (s, 2H), 3.92 (s, 2H), 3.72–3.50 (m, 10H), 3.48–3.44 (m, 2H), 3.41 (t, J = 5.5 Hz, 4H), 3.36 (t, J = 5.5 Hz, 4H), 3.21 (t, J = 5.5 Hz, 2H), 3.10 (s, 3H), 3.01 (s, 3H), 2.78 (t, J = 6.4 Hz, 2H); ^{13}C NMR (125 MHz, CD_3OD) δ (ppm) 172.1, 169.8, 169.2, 164.4, 158.9, 152.8, 152.2, 148.2, 145.0, 144.2, 137.8, 137.0, 135.9, 134.9, 133.9, 131.8, 131.2, 128.2, 127.0, 125.8, 124.6, 123.3, 122.3, 117.9, 116.3, 115.2, 114.4, 113.3, 108.8, 104.7, 98.9, 71.2, 70.3, 70.2, 68.4, 57.9, 54.7, 54.5, 43.6, 43.6, 41.3, 40.3, 40.0, 36.3, 29.9; HRESI-MS (m/z) calcd for $C_{49}H_{57}N_{11}O_7$ ($[M+2H]^{2+}$) 456.7294, found 456.7298.

4.2. CD titration experiment using Ligand 6Q

CD spectrum was measured using a sample solution containing 5.0 μM DNA1 (5.0 μM in A_3T_3 concentration), 3.0 mM HEPES and 3.0 mM NaCl in at pH 7.0 and 25 °C. In the titration experiment, the concentration of Ligand 6Q was varied from 0 to 10 μM (0–2 equiv in regard to A_3T_3). The observed spectral changes are summarized in Figure 3A. Similarly, CD spectrum was measured using a sample solution containing 2.0 μM DNA5(3) (10.0 μM in A_3T_3 concentration), 3.0 mM HEPES and 3.0 mM NaCl at pH 7.0 and 25 °C. In the titration experiment, the concentration of Ligand 6Q was varied from 0 to 20 μM (0–2 equiv in regard to A_3T_3). The observed spectral changes are summarized in Figure 3B. The titration data observed at 275 nm and those at 370 nm were fitted with the non-linear least-square method using Eq. 3, where ΔF_{max} and K_d were optimized.[30]

$$\Delta F = \frac{\Delta F_{max}}{DNA_0}\left(\frac{L_0}{2}+\frac{A}{2}\left(1-\sqrt{\frac{L_0^2-2L_0B}{A^2}+1}\right)\right) \quad (3)$$

$$A = DNA_0 + K_d$$

$$B = DNA_0 - K_d$$

$$\Delta F = \Delta F_H + \Delta F_L \quad (4)$$

$$\Delta F_H = \frac{\Delta F^H_{max}}{DNA_0}\left(\frac{L_0}{2}+\frac{A_H}{2}\left(1-\sqrt{\frac{L_0^2-2L_0B_H}{A_H^2}+1}\right)\right) \quad (5)$$

$$A_H = DNA_0 + K^H_d$$

$$B_H = DNA_0 - K^H_d$$

$$\Delta F_L = \frac{\Delta F^L_{max}}{DNA_0}\left(\frac{L_0}{2}+\frac{A_L}{2}\left(1-\sqrt{\frac{L_0^2-2L_0B_L}{A_L^2}+1}\right)\right) \quad (6)$$

$$A_L = DNA_0 + K^L_d$$

$$B_L = DNA_0 - K^L_d$$

4.3. Fluorescence titration using Ligand Q as a general procedure

A sample solution containing 10 nM Ligand, 3.0 mM HEPES and 3.0 mM NaCl was stirred for 4 h at pH 7.0 and room temperature in

a quartz cell. The fluorescence spectrum was measured with excitation wavelength at 363 nm at 25 °C. In the titration experiment, an aliquot of a DNA solution was added into the sample solution, and whole was stirred for 1 h before measuring fluorescence spectrum. The concentration of DNA was varied from 0 to 0.8 μM (0 to 4 μM in regard to A_3T_3 concentrations). The observed ΔF values were plotted against the A_3T_3 concentration. The observed titration data were well fitted to the theoretical values using Eqs. 4–6 by predicting an appropriate binding stoichiometry. The values of K_d^H, ΔF_{max}^H, K_d^L, and ΔF_{max}^L were calculated by the non-linear curve-fitting method using KaleidaGraph 4.0 J. The ΔF_{max} value was obtained by summing ΔF_{max}^H and ΔF_{max}^L values.

4.4. McGhee–von Hippel analysis of the fluorescence titration data

Based on the predicted ΔF_{max} value obtained as above, the complex concentration was calculated at each DNA concentration. The complex concentration was divided by the base pair concentration to give the ν value. Also, the free ligand concentration (L) was calculated to give the v/L value. The v and v/L values were plotted to produce the Scatchard plot, which is shown in Figure 4B. The v values were used to simulate v/L values by Eq. 1 using three parameters, n, K and ω. The sum of the square values of difference between the observed and the calculated v/L values were optimized by Solver installed in Microsoft Excel. The obtained n, K and ω parameters for Ligand 6Q were used to calculate the ratio of bound ligand per total ligand concentration at each base pair concentration, which is shown in blue line of Figure 4A, demonstrating an excellent agreement to the experimental data. The fluorescence titration experiments were performed using fifteen ligands, and the data were similarly analyzed by the McGhee–von Hippel method to give three parameters. The cooperativity ω values are summarized in Figure 5. All data are summarized in Table S1 in Supporting information.

4.5. UV spectra measurements

A sample solution (200 μL) was stirred for 7 h at room temperature before UV measurement. Final concentrations of sample solutions contain 5 μM Ligand in the absence or presence of 5 μM DNA5(3) in 3.0 mM HEPES, 3.0 mM NaCl, pH 7.0, at 25 °C. The UV spectral changes of Ligand 6Q are summarized in Figure 6A. The Hoechst region Ligand 6Q shifted by binding with DNA5(3) to longer wavelength (372.5–384.5 nm) with 50% increase in the intensity, the quinoline region shifted to shorter wavelength (328.5–326.5 nm) with 43% increase in the intensity (Fig. 6A). The UV spectra of Ligand 6QBr showed similar shifts with smaller changes in intensity (Fig. 6B).

Acknowledgments

We are grateful for support provided by a Grant-in-Aid for Scientific Research (S) (Grant number 21229002) and Restart Postdoctoral Fellowship to JB (Grant number 18 06231) from the Japan Society for the Promotion of Science (JSPS).

Supplementary data

Supplementary data associated with this article can be found, in the online version, at http://dx.doi.org/10.1016/j.bmc.2015.05.056.

References and notes

1. Mirkin, S. M. *Curr. Opin. Struc. Biol.* **2006**, *16*, 351.
2. Shapiro, J. A.; von Sternberg, R. *Biol. Rev. Camb. Philos. Soc.* **2005**, *80*, 227.
3. Rao, S. R.; Trivedi, S.; Emmanuel, D.; Merita, K.; Hynniewta, M. J. *Cell. Mol. Biol.* **2010**, *7*, 1.
4. Brooks, T. A.; Kendrick, S.; Hurley, L. *FEBS J.* **2010**, *277*, 3459.
5. McMurray, C. T. *Nat. Rev. Genet.* **2010**, *11*, 786.
6. Di Prospero, N. A.; Fischbeck, K. H. *Nat. Rev. Genet.* **2005**, *6*, 756.
7. Wang, M.; Law, M.; Duhamel, J.; Chen, P. *Biophys. J.* **2007**, *93*, 2477.
8. Hadadzadeh, H.; Daryanavard, M.; Morshedi, M. *Inorg. Chim. Acta* **2013**, *400*, 82.
9. Gaugain, B.; Barbet, J.; Capelle, N.; Roques, B. P.; Le Pecq, J. B.; Le Bret, M. *Biochemistry* **1978**, *17*, 5078.
10. Guan, Y.; Shi, R.; Li, X.; Zhao, M.; Li, Y. *J. Phys. Chem. B* **2007**, *111*, 7336.
11. Loontiens, F. G.; Regenfuss, P. *Biochemistry* **1990**, *29*, 9029.
12. Haq, I.; Ladbury, J. E.; Chowdhry, B. Z.; Jenkins, T. C.; Chaires, J. B. *J. Mol. Biol.* **1997**, *271*, 244.
13. Gavathiotis, E.; Sharman, G. J.; Searle, M. S. *Nucleic Acids Res.* **2000**, *28*, 728.
14. Liu, Y.; Chai, Y.; Kumar, A.; Tidwell, R. R.; Boykin, D. W.; Wilson, W. D. *J. Am. Chem. Soc.* **2012**, *134*, 5290.
15. Stokke, T.; Steen, H. B. *J. Histochem. Cytochem.* **1985**, *33*, 333.
16. Breusegem, S. Y.; Clegg, R. M.; Loontiens, F. G. *J. Mol. Biol.* **2002**, *315*, 1049.
17. Maiti, S.; Chaudhury, N.; Chowdhury, S. *Biochem. Biophys. Res. Commun.* **2003**, *310*, 505.
18. Tanada, M.; Tsujita, S.; Sasaki, S. *J. Org. Chem.* **2006**, *71*, 125.
19. Tanada, M.; Tsujita, S.; Kataoka, T.; Sasaki, S. *Org. Lett.* **2006**, *8*, 2475–2478.
20. McGhee, J. D.; von Hippel, P. H. *J. Mol. Biol.* **1974**, *86*, 469.
21. Kowalczykowski, S. C.; Paul, L. S.; Lonberg, N.; Newport, J. W.; McSwiggen, J. A. *Biochemistry* **1986**, *25*, 1226.
22. Tessmer, I.; Melikishvili, M.; Fried, M. G. *Nucleic Acids Res.* **2012**, *40*, 8296.
23. Bujalowski, W.; Lohman, T. M.; Anderson, C. F. *Biopolymers* **1989**, *28*, 1637.
24. McKay, S. L.; Haptonstall, B.; Gellman, S. H. *J. Am. Chem. Soc.* **2001**, *123*, 1244.
25. Gomes, L. R.; Low, J. N.; Wardell, J. L.; de Cardoso, L. N. *Acta Crystallogr. C* **2013**, *69*, 191.
26. Ghosh, K.; Adhikari, S.; Chattopadhyay, A. P.; Chowdhury, P. R. *Beilstein J. Org. Chem.* **2008**, *4*, 52.
27. Zhang, J.; Chen, P.; Yuan, B.; Ji, W.; Cheng, Z.; Qiu, X. *Science* **2013**, *342*, 611.
28. Mitra, A.; Seaton, P. J.; Ali, R. A.; Williamsonb, T. *Tetrahedron* **1998**, *54*, 15489.
29. Casabianca, L. B.; de Dios, A. C. *J. Phys. Chem. A* **2004**, *108*, 8505.
30. Wilcox, C. S.; Cowart, M. D. *Tetrahedron Lett.* **1986**, *27*, 5563.